(Preprint) AAS 16-323

THREE-DIMENSIONAL GENERALIZED LOGARITHMIC SPIRALS

Javier Roa*and Jesús Peláez†

The family of generalized logarithmic spirals including a control parameter is extended to the three-dimensional case. The in-plane motion is decoupled from the out-of-plane motion in such a way that the integrals of motion found in the planar problem are still preserved in the three-dimensional case. Designing a low-thrust orbit transfer decomposes in two stages: first, orbits are projected on a reference plane and the planar transfer is solved with a generalized logarithmic spiral. Second, the out-of-plane component of the motion is included in order to target the final orbit. The projection of the three-dimensional transfer orbit on the reference plane is a generalized logarithmic spiral. Arbitrary shape-based laws for the 3D motion can be considered. This paper explores a polynomial and a Fourier series shaping method, together with a polynomial steering law. A fictitious low-thrust sample return mission to Ceres is designed to show the versatility of the method.

INTRODUCTION

During the preliminary phases of mission design fast shaping methods are preferred over more accurate but slower techniques. The mission analyst needs to explore large spaces of parameters with little or no a priori information about the solution. Methods based on analytic solutions are a typical example: the patched-conic technique, for instance, was extensively used during the conception of the planetary Grand Tour that took the *Voyager* spacecraft out of the Solar System.[1,2] Despite ignoring all sources of perturbations the solution was sufficiently close to the actual trajectory for initializing the detailed design phase.

In the last decades electric propulsion systems have progressively been replacing chemical thrusters. Low-thrust solutions are particularly attractive for those applications in which the time of flight can be extended significantly in order to improve the delivered mass fraction. Interplanetary missions such as *Dawn* or *Hayabusa* were powered by electric propulsion. The continuous acceleration due to the thrust changes the dynamics of the spacecraft and a new design paradigm is required. In general, given a thrust profile the equations of motion need to be integrated numerically. The solution lacks an intuitive interpretation and this approach is not convenient for preliminary design. Only particular cases such as the constant radial thrust problem admit fully analytic solutions.

Shape-based methods[3] arose as techniques for fast and approximate design of low-thrust trajectories. Instead of integrating the equations of motion given a thrust profile the trajectory is assumed to

*PhD Candidate, Space Dynamics Group, Technical University of Madrid, Pza. Cardenal Cisneros 3, 28040, Madrid. Student Member AIAA. javier.roa@upm.es
Present address: Jet Propulsion Laboratory, California Institute of Technology, 4800 Oak Grove Drive, Pasadena, CA 91109-8099, USA
†Professor and Head, Space Dynamics Group, Technical University of Madrid, Pza. Cardenal Cisneros 3, 28040, Madrid. Member AIAA.

describe a certain curve, and then the thrust required to follow such trajectory is obtained. Depending on the complexity of the curve closed-form solutions to variables such as the orbital velocity or the time of flight can be found. The simplest curve is the logarithmic spiral. Analyzed in the late 1950's by Bacon[4] and Tsu[5] the motion can be completely solved analytically. But these spirals are of little practical interest because the flight-path angle remains constant along the trajectory. Improving the flexibility also increases the complexity of the solution. Petropoulos and Longuski[6] set a milestone in the area of shape-based methods when they published the exponential sinusoid. This new curve has been proven useful for solving many mission design problems.

Roa and Peláez[7,8] found that solving the equations of motion for the simple thrust profile found by Bacon[4] yields not only logarithmic spirals, but an entire family of solutions that they called generalized logarithmic spirals. The dynamics admit two integrals of motion, generalizations of the conservation of the energy and angular momentum. The spirals are endowed with a collection of properties that make them qualitatively similar to the Keplerian orbits. For example, the sign of the constant of the generalized energy classifies the spirals in elliptic, parabolic and hyperbolic. The spirals have been recently improved by introducing a control parameter,[9] and the spiral Lambert's problem turns out to be surprisingly similar to the unperturbed case.[10] This Paper extends the spirals to the three-dimensional case. The in-plane dynamics are completely decoupled from the out-of-plane motion, which has two clear advantages: first, the integrals of motion are preserved and expressions such as the one for the time of flight are still valid; second, the transversal steering law can be designed at convenience with no effects on the planar motion.

The Paper is organized as follows. First, the equations of motion are derived and the integrals of motion are presented. After a brief summary of the generalized logarithmic spirals we present different control laws and show that the design problem reduces to adjusting four coefficients for the out-of-plane motion, to be solved from a system of linear equations. Finally, a non-planar interplanetary transfer is designed.

DYNAMICS

Let $\mathbf{r} \in \mathbb{R}^3$ be the radiusvector of a particle $\mathscr{P}$, which is the solution to the two-body problem

$$\frac{\mathrm{d}^2\mathbf{r}}{\mathrm{d}t^2} + \frac{\mu}{R^3}\mathbf{r} = \mathbf{a}_\mathrm{p}, \qquad R = \|\mathbf{r}\| \tag{1}$$

perturbed by an acceleration $\mathbf{a}_\mathrm{p}$ due to a given thrust profile. In what follows the problem is normalized so that the gravitational parameter μ becomes unity.

Vector $\mathbf{r}$ can be represented by the set of cylindrical coordinates (r, θ, z). Here r is the distance to the vertical axis, θ denotes the polar angle and z is the out-of-plane component. The inertial frame $\mathcal{I}$ is centered at the origin $\mathscr{O}$ and defined as $\mathcal{I} = \{\mathscr{O}; \mathbf{i}_\mathcal{I}, \mathbf{j}_\mathcal{I}, \mathbf{k}_\mathcal{I}\}$. The climb angle is α. Figure 1 depicts the geometry of the three-dimensional trajectory. The position of the subpoint $\mathscr{P}'$ is given by $\mathbf{r}_\parallel$, so that

$$\mathbf{r}(\theta) = \mathbf{r}_\parallel(\theta) + z(\theta)\,\mathbf{k}_\mathcal{I}$$

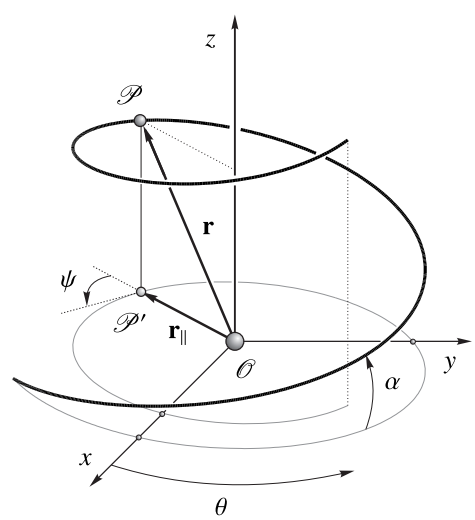

Figure 1: Geometry of a 3D generalized logarithmic spiral

The main hypothesis we adopt is that $\mathbf{r}_{\|}(\theta)$ defines a generalized logarithmic spiral. It is called the *base spiral*. Under this notation it is $\|\mathbf{r}_{\|}\| = r$ and $R^2 = r^2 + z^2$.

Let $\mathcal{F} = \{\mathscr{P}; \mathbf{t}, \mathbf{n}, \mathbf{b}\}$ denote the Frenet-Serret frame, where $\mathbf{t}$ is the unit vector tangent to the trajectory, i.e.

$$\mathbf{t} = \frac{\mathrm{d}\mathbf{r}}{\mathrm{d}s} = \frac{\mathbf{v}}{v}$$

Here s denotes an arclength along the curve. The unit vectors $\mathbf{n}$ and $\mathbf{b}$ are the normal and binormal unit vectors, an relate to each other and to $\mathbf{t}$ thanks to the Frenet-Serret formulas. In particular, the first of the Frenet-Serret formulas provides

$$\mathbf{n} = \frac{1}{\kappa}\frac{\mathrm{d}\mathbf{t}}{\mathrm{d}s}$$

where κ is the nonzero curvature of the trajectory, defined explicitly as

$$\kappa = \left\|\frac{\mathrm{d}\mathbf{t}}{\mathrm{d}s}\right\|$$

The binormal vector completes an orthonormal dextral reference frame,

$$\mathbf{b} = \mathbf{t} \times \mathbf{n}$$

Figure 2 shows the configuration of the Frenet-Serret frame. The auxiliary frame $\mathcal{F}_{\|} = \{\mathscr{P}; \mathbf{t}_{\|}, \mathbf{n}_{\|}, \mathbf{b}_{\|}\}$ is defined so that $(\mathbf{t}_{\|} \cdot \mathbf{t}) = \cos\alpha$ and $(\mathbf{t}_{\|} \cdot \mathbf{k}_{\mathcal{I}}) = 0$. It relates to the Frenet-Serret frame $\mathcal{F}$ by means of a rotation of magnitude α about the normal vector.

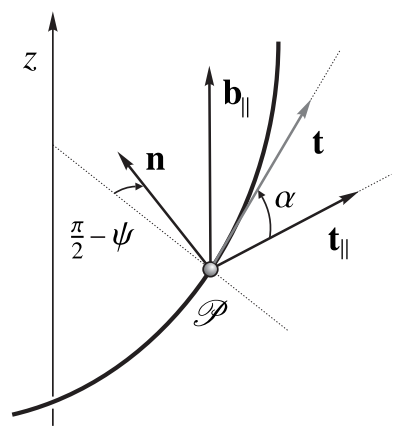

Figure 2: **The Frenet-Serret frame**

The velocity, $\mathbf{v} \in \mathbb{R}^3$, can be decomposed in

$$\mathbf{v} = \mathbf{v}_{\|} + \mathbf{v}_z$$

where $\mathbf{v}_{\|}$ is the in-plane component of the velocity ($\mathbf{v}_{\|} \cdot \mathbf{k}_{\mathcal{I}} = 0$) and the out-of-plane component is $\mathbf{v}_z = \dot{z}\,\mathbf{k}_{\mathcal{I}}$. From the geometry of the problem it follows

$$\frac{\dot{z}}{v_{\|}} = \tan\alpha \implies \frac{\mathrm{d}z}{\mathrm{d}t} = v_{\|}\tan\alpha \tag{2}$$

Taking the time derivative of the out-of-plane velocity defines the transversal acceleration

$$\frac{\mathrm{d}^2 z}{\mathrm{d}t^2} = \tan\alpha\,\frac{\mathrm{d}v_{\|}}{\mathrm{d}t} + v_{\|}\sec^2\alpha\,\frac{\mathrm{d}\alpha}{\mathrm{d}t} \tag{3}$$

The time evolution of $\alpha(t)$ and its derivative are supposed to be known and depend on the shape assumed for the trajectory.

Under the hypothesis that $\mathbf{r}_{\|}$ defines a generalized logarithmic spiral, the equations of motion that govern the in-plane dynamics are those found in Roa and Peláez.[9] When combined with Eqs. (2–3)

it follows the system

$$\frac{\mathrm{d}v_{\|}}{\mathrm{d}t} = \frac{\xi - 1}{r^2}\cos\psi \tag{4}$$

$$\frac{\mathrm{d}r}{\mathrm{d}t} = +v_{\|}\cos\psi \tag{5}$$

$$\frac{\mathrm{d}\theta}{\mathrm{d}t} = +\frac{v_{\|}}{r}\sin\psi \tag{6}$$

$$\frac{\mathrm{d}\psi}{\mathrm{d}t} = \frac{\sin\psi}{r^2 v_{\|}}[2(1-\xi) - r v_{\|}^2] \tag{7}$$

$$\frac{\mathrm{d}z}{\mathrm{d}t} = v_{\|}\tan\alpha \tag{8}$$

$$\frac{\mathrm{d}^2 z}{\mathrm{d}t^2} = \frac{\xi - 1}{r^2}\cos\psi\tan\alpha + v_{\|}(1+\tan^2\alpha)\frac{\mathrm{d}\alpha}{\mathrm{d}t} \tag{9}$$

which needs to be integrated from the initial conditions:

$$t = 0: \quad v_{\|}(t_0) = v_{\|,0}, \quad r(t_0) = r_0, \quad \theta(t_0) = \theta_0, \quad \psi(t_0) = \psi_0, \quad z(t_0) = z_0, \quad \dot{z}(t_0) = \dot{z}_0$$

The control parameter $0 < \xi < 1$ adjusts the magnitude and orientation of the thrust vector. In these equations ψ is the in-plane flight-direction angle, defined as the angle between the projections of the position and velocity vectors onto the $x - y$ plane, i.e.

$$\cos\psi = \frac{(\mathbf{r}_{\|}\cdot\mathbf{v}_{\|})}{r\,v_{\|}} \tag{10}$$

This result refers to the in-plane flight-direction angle. We devote the following lines to finding a similar expression for the absolute flight-direction angle, Ψ, between vectors $\mathbf{r}$ and $\mathbf{v}$.

Let $\{\mathscr{P}; \mathbf{i}, \mathbf{j}, \mathbf{k}\}$ denote the orbital frame $\mathcal{L}$. The unit vectors defining this frame are

$$\mathbf{i} = \frac{\mathbf{r}}{R}, \quad \mathbf{k} = \frac{\mathbf{r}\times\mathbf{v}}{\|\mathbf{r}\times\mathbf{v}\|}, \quad \mathbf{j} = \mathbf{k}\times\mathbf{i}$$

Similarly, consider the orbital frame attached to the subpoint $\mathscr{P}'$, defined in terms of

$$\mathbf{i}_{\|} = \frac{\mathbf{r}_{\|}}{r}, \quad \mathbf{k}_{\|} = \frac{\mathbf{r}_{\|}\times\mathbf{v}_{\|}}{\|\mathbf{r}_{\|}\times\mathbf{v}_{\|}\|}, \quad \mathbf{j}_{\|} = \mathbf{k}_{\|}\times\mathbf{i}_{\|}$$

and denoted $\mathcal{L}'$. The Frenet-Serret frame referred to the projected spiral relates to frame $\mathcal{L}'$ by means of

$$\mathbf{t}_{\|} = \cos\psi\,\mathbf{i}_{\|} + \sin\psi\,\mathbf{j}_{\|}, \qquad \mathbf{n}_{\|} = -\sin\psi\,\mathbf{i}_{\|} + \cos\psi\,\mathbf{j}_{\|}$$

The vectors defining the Frenet-Serret frame attached to the helix admit an equivalent projection onto $\mathcal{L}$:

$$\mathbf{t} = \cos\Psi\,\mathbf{i} + \sin\Psi\,\mathbf{j}, \qquad \mathbf{n} = -\sin\Psi\,\mathbf{i} + \cos\Psi\,\mathbf{j}$$

where Ψ is the flight-direction angle defined by vectors $\mathbf{r}$ and $\mathbf{v}$,

$$\cos\Psi = \frac{(\mathbf{r}\cdot\mathbf{v})}{Rv} \tag{11}$$

We emphasize the difference between this equation and Eq. (10). It then follows

$$\begin{aligned}
\mathbf{t}_{\|} &= \cos\Psi\cos\alpha\,\mathbf{i} + \sin\Psi\cos\alpha\,\mathbf{j} - \sin\alpha\,\mathbf{k} \\
\mathbf{n}_{\|} &= -\sin\Psi\,\mathbf{i} + \cos\Psi\,\mathbf{j} \\
\mathbf{b}_{\|} &= \cos\Psi\sin\alpha\,\mathbf{i} + \sin\Psi\sin\alpha\,\mathbf{j} + \cos\alpha\,\mathbf{k}
\end{aligned}$$

The total velocity of the particle reads

$$\mathbf{v} = v_{\|}\cos\psi\,\mathbf{i}_{\|} + v_{\|}\sin\psi\,\mathbf{j}_{\|} + \dot{z}\,\mathbf{k}_{\|}$$

Provided that $\mathbf{r} = r\,\mathbf{i}_{\|} + z\,\mathbf{k}_{\|}$ Eq. (11) provides

$$\cos\Psi = \frac{rv_{\|}\cos\psi + z\dot{z}}{Rv}$$

The thrust acceleration

The equations of motion (4–9) show that the total acceleration governing the dynamics is

$$\frac{\mathrm{d}^2\mathbf{r}}{\mathrm{d}t^2} = \frac{\xi-1}{r^2}[\cos\psi\,(\mathbf{t}_{\|} + \tan\alpha\,\mathbf{k}_{\mathcal{I}}) - 2\sin\psi\,\mathbf{n}] + v_{\|}\sec^2\alpha\frac{\mathrm{d}\alpha}{\mathrm{d}t}\,\mathbf{k}_{\mathcal{I}}$$

The gravitational acceleration is known to be

$$\mathbf{a}_{\mathrm{g}} = -\frac{\mathbf{r}}{R^3} = -\frac{1}{R^3}\left[r(\cos\psi\,\mathbf{t}_{\|} - \sin\psi\,\mathbf{n}) + z\,\mathbf{k}_{\mathcal{I}}\right]$$

The acceleration due to the thrust decomposes in $\mathbf{a}_{\mathrm{p}} = \mathbf{a}_{\mathrm{p},\|} + \mathbf{a}_{\mathrm{p},z}$. The in-plane component takes the form

$$\mathbf{a}_{\mathrm{p},\|} = \left(\frac{\xi-1}{r^3} + \frac{1}{R^3}\right)r\cos\psi\,\mathbf{t}_{\|} + \left[\frac{2(1-\xi)}{r^3} - \frac{1}{R^3}\right]r\sin\psi\,\mathbf{n}$$

whereas the out-of-plane component of the acceleration reduces to

$$\mathbf{a}_{\mathrm{p},z} = \left[\frac{\xi-1}{r^2}\cos\psi\tan\alpha + v_{\|}\frac{\mathrm{d}}{\mathrm{d}t}(\tan\alpha) + \frac{z}{R^3}\right]\mathbf{k}_{\mathcal{I}} \tag{12}$$

The climb-angle α and its rate of change are known, given the shape of the trajectory. The previous expression is directly referred to $\tan\alpha$ in order to simplify the introduction of a steering law.

When the motion is confined to the plane it is $z = 0$ and $\alpha = 0$. This condition makes $r \equiv R$, and the perturbing acceleration reduces to

$$\mathbf{a}_{\mathrm{p}} = \frac{1}{r^2}[\xi\cos\psi\,\mathbf{t} + (1-2\xi)\sin\psi\,\mathbf{n}] \qquad (z = 0, \alpha = 0)$$

Note that $\mathbf{t} \equiv \mathbf{t}_{\|}$ in this case. The perturbation reduces to the acceleration that generates the family of controlled generalized logarithmic spirals.

Integrals of motion

Combining Eqs. (4) and (5) yields an equation of separate variables

$$\frac{\mathrm{d}v_\parallel}{\mathrm{d}r} = \frac{\xi - 1}{r^2 v_\parallel} \implies v_\parallel \, \mathrm{d}v_\parallel = (\xi - 1)\frac{\mathrm{d}r}{r^2}$$

that is integrated easily to define a first integral of the motion

$$v_\parallel^2 - \frac{2(1-\xi)}{r} = K_1 \tag{13}$$

Here K_1 is the constant of the generalized energy for the planar motion, defined by the initial conditions

$$K_1 = v_{\parallel,0}^2 - \frac{2(1-\xi)}{r_0}$$

The value of the constant K_1 defines the type of the base spiral. If $K_1 < 0$ the base spiral is *elliptic*. Since K_1 is negative and $v_{\parallel,0}^2$ is always positive there is a maximum radius that the base spiral can reach. For $K_1 > 0$ the base spiral is *hyperbolic*; the particle will escape to infinity along an asymptotic branch, reaching $r \to \infty$ with a finite, nonzero velocity. The limit case $K_1 = 0$ yields *parabolic* base spirals, that turn out to be logarithmic spirals. In this case the presence of the control parameter affects the velocity in the logarithmic spiral.

Combining Eqs. (6) and (7) leads to

$$\frac{\mathrm{d}}{\mathrm{d}t}(\psi + \theta) = \frac{2(1-\xi)}{r^2 v_\parallel} \sin\psi$$

Dividing this expression by Eq. (4) yields the differential equation:

$$\mathrm{d}(\psi + \theta) = -\frac{2}{v_\parallel} \tan\psi \, \mathrm{d}v_\parallel$$

The expression for the radial velocity can then be introduced in Eq. (6) and defines the differential $\mathrm{d}\theta$ in terms of $\mathrm{d}r$. With this, the previous equation transforms into

$$\cot\psi \, \mathrm{d}\psi + \frac{\mathrm{d}r}{r} + \frac{2}{v_\parallel}\mathrm{d}v_\parallel = 0$$

Integrating this equation of separate variables renders an integral of motion

$$\ln(\sin\psi) + \ln r + \ln v_\parallel^2 = C$$

where C is a constant of integration. This equation reduces to

$$r v_\parallel^2 \sin\psi = K_2 \tag{14}$$

The constant of motion K_2 is a generalization of the angular momentum of the planar motion. It is solved from

$$K_2 = r_0 v_{\parallel,0}^2 \sin\psi_0$$

It is worth noticing that it does not depend on the value of the control parameter ξ.

The first integrals (13) and (14) show that the flight-direction angle evolves according to

$$\sin\psi = \frac{K_2}{2(1-\xi)+K_1 r} \tag{15}$$

It is also

$$\cos\psi = \pm\frac{\sqrt{[2(1-\xi)+K_1 r]^2 - K_2^2}}{2(1-\xi)+K_1 r} \tag{16}$$

The sign in this expression depends on the regime of the spiral: for spirals in raising regime ($\dot{r} > 0$) it is $\psi < \pi/2$ and therefore $\cos\psi > 0$; on the contrary, for spirals in lowering regime ($\dot{r} < 0$) it is $\psi > \pi/2$ and $\cos\psi < 0$

We emphasize that the integrals of motion found in this section are preserved no matter how $\alpha(t)$ is defined. This phenomenon effectively decouples the in-plane motion from the transversal dynamics.

One of the main advantages of having decoupled the in-plane dynamics is that the expressions for the time of flight (see the following section) still hold. Clearly the time of flight to $\mathscr{P}$ in the absolute motion is the same as the time to $\mathscr{P}'$ in the in-plane case. The time of flight is then given by the expressions defining the time of flight in the base spiral. The only precaution is that the variables that appear in the definition of the time should be referred to the in-plane motion.

GENERALIZED LOGARITHMIC SPIRALS

Before solving the three-dimensional motion we summarize the key concepts of the family of (controlled) generalized logarithmic spirals. We present the equations of the trajectory and time of flight so the reader will find the paper to be self-contained. A more detailed analysis of the solution can be found in the work by Roa and Peláez.[7,8,9] In these papers it is shown that the transition between the different families is continuous. In this section we omit the subscript $\|$ for clarity, but all variables refer to the in-plane motion.

Symmetries

Two types of symmetries can be found in the family of generalized logarithmic spirals. They help to understand the dynamics and simplify the derivation of the solution.

The $\mathscr{T}$-symmetry is a intrinsic property of the trajectory. A curve $r(\theta)$ is said to be $\mathscr{T}$-symmetric if $r(\theta_\mathrm{m}+\delta) = r(\theta_\mathrm{m}-\delta)$ for any $\delta > 0$. We anticipate that only elliptic spirals and one subfamily of hyperbolic spirals are $\mathscr{T}$-symmetric. The axis of $\mathscr{T}$-symmetry is the spiral equivalent to the line of apses and its orientation is given by θ_m.

The $\mathscr{C}$-symmetry is a property of dynamical nature. It appears when comparing two trajectories, but it is not an intrinsic property of one trajectory. Two spirals are said to be $\mathscr{C}$-symmetric if they share the same values of K_1 and K_2. The fact that two different trajectories originate from the same values of the constants of motion can be understood from the first integral (14). The constant K_2 is defined by means of $\sin\psi_0$, which is symmetric with respect to $\psi_0 = \pi/2$. The trajectories departing with $\psi_0 = \pi/2 \pm \delta$ are $\mathscr{C}$-symmetric.

Elliptic spirals

Elliptic spirals never to escape the gravitational well of the attracting body. This yields the existence of a maximum radius

$$r_{\max} = \frac{2(1-\xi) - K_2}{(-K_1)}$$

which is called the apoapsis of the spiral. The condition $K_2 < 2(1-\xi)$ is satisfied naturally because of how $\sin\psi$ is defined in Eq. (15). The velocity at apoapsis is minimum,

$$v_{\mathrm{m}} = \sqrt{\frac{K_2}{r_{\max}}} = \sqrt{\frac{-K_1 K_2}{2(1-\xi) - K_2}}$$

In the limit $K_1 \to 0$ the maximum goes to infinity: this shows that logarithmic spirals can be seen as a limit case of elliptic spirals, that approach infinity along a spiral branch.

The trajectory is given by

$$\frac{r(\theta)}{r_{\max}} = \frac{1 + K_2}{1 + K_2 \cosh\beta(\theta)}$$

having introduced the spiral anomaly:

$$\beta(\theta) = \frac{\ell}{K_2}(\theta - \theta_{\mathrm{m}}), \qquad \text{with } \ell = \sqrt{4(1-\xi)^2 - K_2^2}$$

The angle θ_{m} is the orientation of the apoapsis and can be solved from the initial conditions

$$\theta_{\mathrm{m}} = \theta_0 \pm \frac{K_2}{\ell}\left|\operatorname{arccosh}\left\{\frac{r_{\max}}{r_0} - \frac{2(1-\xi)}{K_2}\left(1 - \frac{r_{\max}}{r_0}\right)\right\}\right|$$

The first sign is chosen if the spiral is initially in raising regime, and the second if it is lowering regime.

The time of flight is written as a function of the radial distance:

$$t(r) - t_{\mathrm{m}} = \pm\frac{rv}{K_1}\sqrt{\frac{1-\sin\psi}{1+\sin\psi}} \pm \frac{2[2(1-\xi)k'^2\Delta\Pi - K_2\Delta\mathrm{E}]\sqrt{1-\xi}}{(-K_1)^{3/2}\sqrt{K_2}}$$

It is referred to the time of passage through the apoapsis $r_{\max}$, denoted t_{m}. The solution is given in terms of the complete and the incomplete elliptic integrals of the second, $\mathrm{E}(\phi, k)$, and third kinds, $\Pi(p; \phi, k)$, namely:

$$\Delta\mathrm{E} = \mathrm{E}(\phi, k) - \mathrm{E}(k), \qquad \Delta\Pi = \Pi(p; \phi, k) - \Pi(p; k)$$

Their argument, modulus and parameter are, respectively:

$$\sin\phi = \frac{v_{\mathrm{m}}}{v}\sqrt{\frac{2}{1+\sin\psi}}, \qquad k = \sqrt{\frac{-K_1 r_{\max}}{4(1-\xi)}}, \qquad p = \frac{K_1 r_{\max}}{2K_2}$$

The complementary modulus k' is defined as $k' = \sqrt{1-k^2}$.

The time of apoapsis passage t_{m} is computed initially from the initial conditions:

$$t_{\mathrm{m}} = \mp\frac{r_0 v_0}{K_1}\sqrt{\frac{1-\sin\psi_0}{1+\sin\psi_0}} \mp \frac{2[2(1-\xi)k'^2\Delta\Pi_0 - K_2\Delta\mathrm{E}_0]\sqrt{1-\xi}}{(-K_1)^{3/2}\sqrt{K_2}}$$

The first sign corresponds to raising regime, and the second to lowering regime.

Parabolic spirals

When K_1 vanishes the velocity in the spiral reduces to

$$v = \sqrt{\frac{2(1-\xi)}{r}}$$

It is straightforward to verify that the velocity when reaching infinity along the spiral branch goes to zero.

The trajectory is simply

$$r(\theta) = r_0\, \mathrm{e}^{(\theta-\theta_0)\cot\psi}$$

Equation (15) shows that the flight-direction angle remains constant. Combining this equation with Eq. (16) it follows

$$\cot\psi = \pm\frac{\ell}{K_2}$$

The parameter $\ell = \sqrt{4(1-\xi)^2 - K_2^2}$ remains as defined for the elliptic case.

The time of flight reduces to

$$t(r) - t_0 = \pm\frac{2\sqrt{2(1-\xi)}}{3\ell}(r^{3/2} - r_0^{3/2})$$

It is referred directly to the initial conditions and requires no further computations.

Hyperbolic spirals

Hyperbolic spirals are defined by $K_1 > 0$, which makes

$$v_\infty^2 = K_1$$

The constant K_1 is equivalent to the characteristic energy C_3.

The are two types of hyperbolic spirals: Type I spirals, $K_2 < 2(1-\xi)$, only have one asymptote, which means that a spiral in raising regime escapes and a spiral in lowering regime falls to the origin; Type II spirals, $K_2 > 2(1-\xi)$, have two asymptotes. The particle approaches the origin from an asymptote, reaches a minimum radius $r_{\min} \neq 0$, transitions to raising regime and then escapes along a symmetric asymptote.

Hyperbolic spirals of Type I Since there are no axes of symmetry in this family of solutions the spiral anomaly is redefined with respect to the orientation of the asymptote as

$$\beta(\theta) = \pm\frac{\ell}{K_2}(\theta_{\mathrm{as}} - \theta)$$

Here θ_{as} defines the asymptote. It is defined from the initial conditions

$$\theta_{\mathrm{as}} = \theta_0 \pm \frac{K_2}{\ell}\ln\left[\frac{K_2(\zeta - \ell - K_2\sin\psi_0 + \ell\,|\cos\psi_0|)}{r_0 K_1 \zeta \sin\psi_0}\right] \tag{17}$$

in terms of the parameter $\zeta = 2(1-\xi) + \ell$.

The equation of the trajectory is

$$r(\theta) = \frac{\zeta \ell^2 / K_1}{\sinh \frac{\beta}{2} \left[4\zeta(1-\xi) \sinh \frac{\beta}{2} + (\zeta^2 - K_2^2) \cosh \frac{\beta}{2} \right]}$$

The trajectory depends on the regime of the spiral through $\beta(\theta)$. Note that the orientation of the asymptote is also affected by the initial regime.

The time of flight for the case $K_1 > 0$ and $K_2 < 2(1-\xi)$ becomes

$$t(r) = K_4 \pm \left\{ \frac{rv}{K_1} \sqrt{\frac{1+\sin\psi}{1-\sin\psi}} - \frac{2\left\{\mathrm{E} - (1-p)\Pi\right\} \sqrt{K_2(1-\xi)}}{K_1^{3/2}} \right\}$$

written in terms of a constant K_4, which is easily solved by particularizing the previous equation at $t = 0$. The solution is given in terms of the incomplete elliptic integrals of the second and third kinds, $\mathrm{E} = \mathrm{E}(\phi, k)$ and $\Pi = \Pi(p; \phi, k)$, with:

$$\sin\phi = \sqrt{\frac{K_1 r \sin\psi}{p K_2 (1-\sin\psi)}}, \qquad k = \frac{1}{2}\sqrt{\frac{2(1-\xi)+K_2}{1-\xi}}, \qquad p = \frac{2(1-\xi)+K_2}{2K_2}$$

Hyperbolic spirals of Type II The periapsis radius takes the form

$$r_{\min} = \frac{K_2 - 2(1-\xi)}{K_1}$$

The velocity at periapsis is the maximum velocity in the spiral and reads

$$v_{\mathrm{m}} = \sqrt{\frac{K_2}{r_{\min}}} = \sqrt{\frac{K_1 K_2}{K_2 - 2(1-\xi)}}$$

The periapsis of the spiral defines an axis of $\mathscr{T}$-symmetry, oriented as θ_{m}:

$$\theta_{\mathrm{m}} = \theta_0 \mp \frac{K_2}{\ell} \left\{ \frac{\pi}{2} + \arctan\left[\frac{2(1-\xi) - K_2 \sin\psi_0}{\ell \,|\cos\psi_0|} \right] \right\}$$

As always, the first sign corresponds to raising regime and the second to lowering regime. With this angle the spiral anomaly is defined as

$$\beta(\theta) = \frac{\ell}{K_2}(\theta - \theta_{\mathrm{m}})$$

The parameter ℓ is redefined as $\ell = \sqrt{K_2^2 - 4(1-\xi)^2}$ for the signs to be compatible.

The equation of the trajectory is

$$\frac{r(\theta)}{r_{\min}} = \frac{2(1-\xi)+K_2}{2(1-\xi)+K_2\cos\beta(\theta)}$$

Due to the denominator in this expression two asymptotes appear naturally:

$$\theta_{\mathrm{as}} = \theta_{\mathrm{m}} \pm \frac{K_2}{\ell} \left\{ \frac{\pi}{2} + \arctan\left[\frac{2(1-\xi)}{\ell} \right] \right\}$$

The particle escapes to infinity along the asymptote defined by the (+) sign, and comes from infinity along the asymptote defined by the (−) sign.

Finally, the time of flight reads

$$t(r) - t_{\mathrm{m}} = \mp \left\{ \frac{[K_2 + 2(1-\xi)]K_2\mathrm{E} - K_1 r_{\min}[K_2\mathrm{F} + 2(1-\xi)\Pi]}{K_1\sqrt{K_1K_2[K_2+2(1-\xi)]}} \right.$$
$$\left. + \frac{2(1-\xi)}{K_1^{3/2}} \operatorname{arcsinh}\left[\frac{\sqrt{2K_1 r(rv^2 - K_2)}}{2\sqrt{K_2 rv^2 + (rv^2 - K_2)(1-\xi)}}\right] - \frac{v}{K_1^2}\sqrt{r^2v^4 - K_2^2}\right\} \tag{18}$$

It is given in terms of the incomplete elliptic integrals of the first, $\mathrm{F} \equiv \mathrm{F}(\phi, k)$, second, $\mathrm{E} \equiv \mathrm{E}(\phi, k)$, and third kinds, $\Pi \equiv \Pi(p; \phi, k)$. The argument of the elliptic integrals in this case is

$$\sin\phi = \frac{\sqrt{2(1-\xi)(1-\sin\psi)}}{k\sqrt{K_2 - 2(1-\xi)\sin\psi}}, \qquad k = \frac{2\sqrt{1-\xi}}{\sqrt{K_2 + 2(1-\xi)}}, \qquad p = \frac{2(1-\xi)}{K_2}$$

The time of periapsis passage t_{m} can be easily solved from Eq. (18) particularized at $t = 0$.

Transition between Type I and Type II hyperbolic spirals Hyperbolic spirals of Type I have been defined for $K_2 < 2(1-\xi)$, whereas $K_2 > 2(1-\xi)$ yields hyperbolic spirals of Type II. In the limit case $K_2 = 2(1-\xi)$ the equations of motion simplify noticeably; the resulting spiral is

$$r(\theta) = \frac{4(1-\xi)}{K_1\beta(\beta \mp 2)}$$

In this case the angular variable $\beta(\theta)$ is defined with respect to the orientation of the asymptote. That is

$$\beta = \theta - \theta_{\mathrm{as}}$$

The asymptote is fixed by

$$\theta_{\mathrm{as}} = \theta_0 \mp \left[1 - \sqrt{1 + \frac{4(1-\xi)}{K_1 r_0}}\right]$$

The time of flight is no longer given by elliptic integrals. It reduces to

$$t(r) - t_0 = \pm\frac{1}{K_1^{3/2}}\left\{\Xi - \Xi_0 + (1-\xi)\ln\left[\frac{r_0 v_0^2 + 1 - \xi + \Xi_0}{rv^2 + 1 - \xi + \Xi}\right]\right\}$$

The auxiliary parameter $\Xi = \Xi(r)$ reads

$$\Xi(r) = v\sqrt{r[rv^2 + 2(1-\xi)]}$$

The equation for the time of flight has been referred directly to the initial conditions for convenience.

SOLUTION TO THE OUT-OF-PLANE MOTION

Helices

The simplest law for the evolution of the climb-angle α is

$$\alpha = \text{const.}$$

and of course its time derivative is nil. The radial velocity has been defined in Eq. (5) as the projection of the velocity along the direction of $\mathbf{r}_{\|}$. Combining this expression with Eq. (2) yields

$$\frac{\mathrm{d}z}{\mathrm{d}r} = \frac{\tan\alpha}{\cos\psi} \tag{19}$$

The term $\cos\psi$ has already been defined explicitly in Eq. (16). It is interesting to see that the sign of this expression depends on the regime of the spiral through the sign of $\cos\psi$. It becomes

$$\frac{\mathrm{d}z}{\mathrm{d}r} = \pm\frac{[2(1-\xi)+K_1 r]\tan\alpha}{\sqrt{[2(1-\xi)+K_1 r]^2 - K_2^2}} \tag{20}$$

This equation shows that the out-of-plane motion can be solved in closed-form when the angle α is constant, being:

$$z(r) - z_0 = \frac{K_2}{K_1}\tan\alpha(\cot\psi - \cot\psi_0) \tag{21}$$

Recall that

$$\tan\psi = \pm\frac{K_2}{\sqrt{[2(1-\xi)+K_1 r]^2 - K_2^2}}$$

The constant K_1 appears in the denominator of the solution in Eq. (21). In the limit case $K_1 \to 0$ this expression will become singular. But the singularity is avoidable as shown by the limit

$$\lim_{K_1\to 0} z(r) = z_0 + 2(r - r_0)(1-\xi)\tan\alpha\sec\psi_0$$

When $K_1 = 0$ the spiral is parabolic (logarithmic) and the flight-direction angle remains constant, $\psi = \psi_0$.

Figure 3 shows examples of different helicoidal trajectories depending on the type of the corresponding base spiral. By extension we call elliptic helices those helices whose base spiral is elliptic. The same applies to parabolic and hyperbolic helices. Elliptic helices resemble spherical spirals, the poles corresponding to $r \to 0$ in the base spiral. Parabolic helices evolve on the surface of a cone.

The geometry of the problem is such that

$$(\mathbf{t}\cdot\mathbf{k}_I) = \sin\alpha$$

Taking the derivative with respect to the arclength, s, provides

$$\left(\frac{\mathrm{d}\mathbf{t}}{\mathrm{d}s}\cdot\mathbf{k}_I\right) = 0 \tag{22}$$

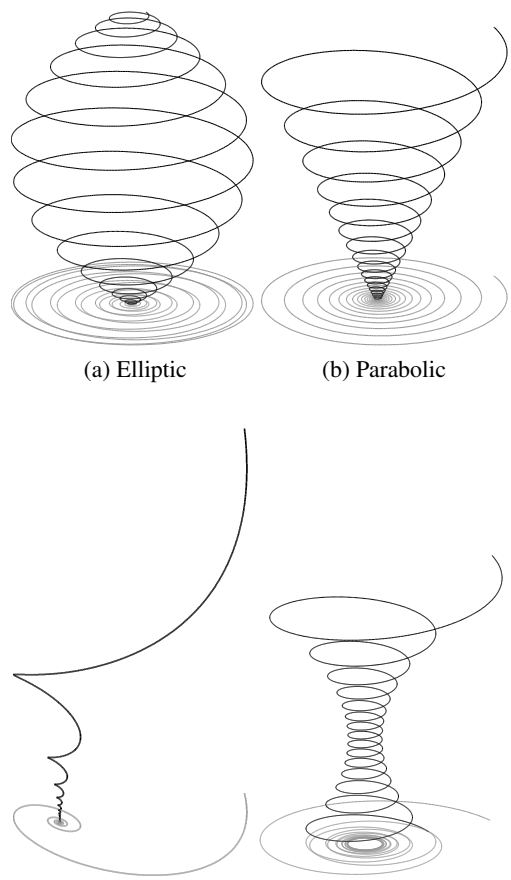

Figure 3: **Helicoidal trajectories depending on the type of base spiral**

The derivative of $\mathbf{t}$ with respect to the arclength relates to $\mathbf{n}$ by means of the first of the Frenet-Serret formulas,

$$\frac{\mathrm{d}\mathbf{t}}{\mathrm{d}s} = \kappa\,\mathbf{n}$$

Therefore, Eq. (22) translates into

$$\kappa\,(\mathbf{n}\cdot\mathbf{k}_{\mathcal{I}}) = 0$$

so vector $\mathbf{n}$ is confined to the plane defined by $\mathbf{k}_{\mathcal{I}}$, provided that the helix has nonzero curvature. This proves that the normal vector of a generalized logarithmic helix $\mathbf{n}$ is always parallel to the $x-y$ plane.

From a geometric perspective it is interesting to prove that the resulting curve satisfies the condition for a curve being a helix, given by Lancret's theorem. It states that a curve is called a helix if the ratio between the curvature, κ, and the torsion, τ, is constant.* The axis of the helix is defined by the unit vector $\mathbf{k}_{\mathcal{I}}$, and can be referred to the Frenet-Serret frame by virtue of

$$\mathbf{k}_{\mathcal{I}} = \sin\alpha\,\mathbf{t} + \cos\alpha\,\mathbf{b}$$

Differentiating with respect to the arclength s yields

$$0 = \sin\alpha\left(\frac{\mathrm{d}\mathbf{t}}{\mathrm{d}s}\right) + \cos\alpha\left(\frac{\mathrm{d}\mathbf{b}}{\mathrm{d}s}\right)$$

The Frenet-Serret formulas transform this expression into

$$\kappa(s)\sin\alpha\,\mathbf{n} - \tau(s)\cos\alpha\,\mathbf{n} = 0 \implies \frac{\kappa(s)}{\tau(s)} = \cot\alpha$$

so that the ratio κ/τ is indeed constant when $\alpha = \text{const}$.

The connection between Eq. (21) and the initial conditions (z_0, ψ_0) comes from solving for the constant of integration given the departure point. Without losing generality the constant of integration can be obtained from the conditions at apoapsis or periapsis when the spiral is either elliptic or hyperbolic of Type II. This provides a new form of the equation of the trajectory:

$$z(r) - z_{\mathrm{m}} = \frac{K_2\tan\alpha}{K_1\tan\psi} \tag{23}$$

Here $z_{\mathrm{m}} = z(r_{\mathrm{max}})$ or $z_{\mathrm{m}} = z(r_{\mathrm{min}})$, depending on whether the helix is elliptic or hyperbolic of Type II.

This suggests a new concept of symmetry: a generalized helix is said to be $\mathscr{Z}$-symmetric if

$$z(\theta_{\mathrm{m}} + \Delta) = -z(\theta_{\mathrm{m}} - \Delta)$$

where $\Delta \geq 0$ denotes an arbitrarily large angular displacement. The component z depends on the polar angle through the relations $r = r(\theta)$ and $\psi = \psi(\theta)$. $\mathscr{Z}$-symmetric trajectories are invariant

*This theorem was first presented by the engineer Michel A. Lancret in *Mémoire sur les courbes à double courbure*, on April 26, 1802. But the formal proof of the theorem is attributed to Saint Venant, published in his *Mémoire sur les lignes courbes non planes* in 1845. He worked with the concept of the rectifying plane (spanned by vectors $\mathbf{t}$ and $\mathbf{b}$): by evaluating the relative inclination of the line of intersection between consecutive rectifying planes he proved that for a helix such lines are parallel. Moreover, they describe a cylinder. He then reduced the condition for the rectifying lines to be parallel to $\mathrm{d}(\kappa/\tau) = 0$. We refer to Barros[11] for a generalization of Lancret's theorem.

with respect to rotations of magnitude $\vartheta = n\pi$ (with $n = 1, 2, \ldots$) about the axis $\theta = \theta_\mathrm{m}$ located in the $z = z_\mathrm{m}$ plane. Clearly a $\mathscr{Z}$-symmetric trajectory is $\mathscr{T}$-symmetric, because a maximum or minimum radius exists. Similarly, all $\mathscr{T}$-symmetric trajectories are $\mathscr{Z}$-symmetric because Eq. (23) will always change its sign when ψ reaches $\pi/2$.

Elliptic spirals are known to be bounded, so that $r \to 0$ when $\theta \to \pm\infty$. Similarly, Eq. (23) proves that the out-of-plane motion is also bounded:

$$\lim_{r\to 0} z(r) = z_\mathrm{m} \pm \frac{\ell}{K_1} \tan\alpha$$

This result clearly shows the $\mathscr{Z}$-symmetry of the helix.

On the contrary, for the case of parabolic and hyperbolic spirals the particle escapes to infinity. This means $\lim_{r\to\infty} z(r) = \pm\infty$ depending on the type and regime of the helix. For hyperbolic helices of Type II there are two asymptotes that provide $z \to \pm\infty$.

Polynomial shape

Following the shape-based approach the out-of-plane component of the motion can be modeled as

$$z(\theta) = \sum_{n=0}^{N} c_n \theta^n$$

The shape coefficients c_n are stored in the vector $\mathbf{c}_N \in \mathbb{R}^{N+1}$. The transversal velocity follows from the relation

$$\frac{\mathrm{d}z}{\mathrm{d}t} = \frac{\mathrm{d}z}{\mathrm{d}\theta}\frac{\mathrm{d}\theta}{\mathrm{d}t} = \frac{v_\parallel}{r}\sin\psi \sum_{n=1}^{N} n c_n \theta^{n-1} \tag{24}$$

having introduced Eq. (6).

The steering law $\alpha(\theta)$ can be solved by equating Eqs. (24) and (2):

$$\tan\alpha = \frac{\sin\psi}{r}\sum_{n=1}^{N} n c_n \theta^{n-1}$$

The transversal component of the thrust acceleration, given in Eq. (12), involves the time derivative of $\tan\alpha$:

$$\frac{\mathrm{d}}{\mathrm{d}t}(\tan\alpha) = \frac{\mathrm{d}}{\mathrm{d}t}\left(\frac{\sin\psi}{r}\right)\sum_{n=1}^{N} n c_n \theta^{n-1} + \frac{v_\parallel \sin^2\psi}{r^2}\sum_{n=2}^{N} n(n-1) c_n \theta^{n-2}$$

This solution requires an expression for $\mathrm{d}(\sin\psi/r)/\mathrm{d}t$, which takes the form

$$\frac{\mathrm{d}}{\mathrm{d}t}\left(\frac{\sin\psi}{r}\right) = -\frac{\sin\psi\cos\psi}{r^2 v_\parallel}(K_1 + v_\parallel^2) \tag{25}$$

Fourier series

Consider the alternative shape of the transversal component of the motion, modeled by a Fourier series:

$$z(\theta) = a_0 + \sum_{n=1}^{N}[a_n \cos(n\theta) + b_n \sin(n\theta)]$$

The out-of-plane velocity takes the form

$$\frac{\mathrm{d}z}{\mathrm{d}t} = -\frac{v_\parallel}{r}\sin\psi \sum_{n=1}^{N}\{n[a_n\sin(n\theta) - b_n\cos(n\theta)]\}$$

Similarly, the steering law becomes

$$\tan\alpha = -\frac{\sin\psi}{r}\sum_{n=1}^{N}\{n[a_n\sin(n\theta) - b_n\cos(n\theta)]\}$$

Its time derivative, required for computing the out-of-plane acceleration, is

$$\frac{\mathrm{d}}{\mathrm{d}t}(\tan\alpha) = -\frac{\mathrm{d}}{\mathrm{d}t}\left(\frac{\sin\psi}{r}\right)\sum_{n=1}^{N}\{n[a_n\sin(n\theta) - b_n\cos(n\theta)]\} - \frac{v_\parallel\sin^2\psi}{r^2}\sum_{n=1}^{N}\{n^2[a_n\cos(n\theta) + b_n\sin(n\theta)]\}$$

The derivative that appears in the first term is given in Eq. (25).

TRANSFERS BETWEEN ARBITRARY ORBITS

The method for designing transfers between arbitrary orbits consists in two steps:

1. The target orbit is projected on the orbital plane of the departure orbit. The transfer between the departure orbit and the projection of the target orbit is solved using a generalized logarithmic spiral. This defines the in-plane components of the motion, the time of flight, the control parameter ξ, and the constants of motion K_1 and K_2.

2. The out-of-plane motion is designed to satisfy the boundary conditions at departure and arrival. If the polynomial law from the previous section is used, the problem reduces to adjusting the values of the coefficients c_n. A similar approach is followed when implementing the Fourier shape, by solving for a_n and b_n.

Given the initial conditions $(z_0, \dot{z}_0)$ two of the shape coefficients need to be adjusted in order the trajectory to satisfy $z(r_0) = z_0$ and $\dot{z}(r_0) = \dot{z}_0$. These equations are linear in the coefficients c_i. Let $(z_\mathrm{f}, \dot{z}_\mathrm{f})$ be the arrival conditions for the out-of-plane motion. The boundary conditions provide the relation $z_\mathrm{f} = z(r_\mathrm{f})$, where r_f is the value of the cylindrical radius at the arrival point and $z(r)$ is the assumed law for the evolution of z. The conditions on the velocity render $\dot{z}_\mathrm{f} = \dot{z}(r_\mathrm{f})$. The problem imposes a total of four constraints to the system: the trajectory is forced to depart from $(z_0, \dot{z}_0)$ and to arrive to $(z_\mathrm{f}, \dot{z}_\mathrm{f})$. At least four shape coefficients are required.

Polynomial shape

One simple approach is to solve for the first four coefficients $n = 0, \ldots, 3$, stored in $\mathbf{c}_3$. But different strategies can be adopted depending on the number of coefficients. The linear system of equations can be written in matrix form as

$$\mathbf{Z} = \mathbf{M}\,\mathbf{c}_3 + \mathbf{N}\,\mathbf{c}_{4:N}$$

The boundary conditions are stored in the vector $\mathbf{Z} = (z_0, z_\mathrm{f}, \dot{z}_0, \dot{z}_\mathrm{f})^\top$. Vector $\mathbf{c}_{4:N}$ refers to the remaining coefficients not included in $\mathbf{c}_3$, and the matrices $\mathbf{M} \in \mathbb{R}^{4\times4}$ and $\mathbf{N} \in \mathbb{R}^{4\times(N-4)}$ depend on

the shape function. Denoting M_n the $(n+1)$-th column of matrix $\mathbf{M}$, and N_m the $(m+1)$-th column of matrix $\mathbf{N}$, it follows:

$$M_n = \begin{bmatrix} \theta_0^n \\ \theta_\mathrm{f}^n \\ n\theta_0^{n-1}C_0 \\ n\theta_\mathrm{f}^{n-1}C_\mathrm{f} \end{bmatrix} \qquad \text{and} \qquad N_m = \begin{bmatrix} \theta_0^m \\ \theta_\mathrm{f}^m \\ m\theta_0^{m-1}C_0 \\ m\theta_\mathrm{f}^{m-1}C_\mathrm{f} \end{bmatrix}$$

with $n = 0, \ldots, 3$ and $m = 4, \ldots, N$. For simplicity the coefficient $C = v_\parallel \sin\psi / r$ has been introduced.

The matrix equation can be solved for $\mathbf{c}_3$ to provide

$$\mathbf{c}_3 = \mathbf{M}^{-1}(\mathbf{Z} - \mathbf{N}\,\mathbf{c}_{4:N})$$

The determinant of matrix $\mathbf{M}$ is

$$\Delta = -C_0 C_\mathrm{f}(\theta_\mathrm{f} - \theta_0)^4$$

It will only vanish if $\theta_0 = \theta_\mathrm{f}$ or $C_j = 0$. The former is not possible since θ always grows in time. The latter only occurs when $\psi \to 0$ (degenerate rectilinear orbit) or $r \to \infty$ (escape); both situations are limit cases that are omitted for consistency. Under these hypotheses the matrix $\mathbf{M}$ is regular.

Fourier series

When considering the Fourier series representation the boundary conditions can be written

$$\mathbf{Z} = \mathbf{M}\,\mathbf{c} + \mathbf{C}$$

Vector $\mathbf{c}$ groups the coefficients (a_0, a_1, b_1, a_2) and matrix $\mathbf{M}$ reads

$$\mathbf{M} = \begin{bmatrix} 1 & \cos\theta_0 & \sin\theta_0 & \cos 2\theta_0 \\ 1 & \cos\theta_\mathrm{f} & \sin\theta_\mathrm{f} & \cos 2\theta_\mathrm{f} \\ 0 & -C_0\sin\theta_0 & C_0\cos\theta_0 & -2C_0\sin 2\theta_0 \\ 0 & -C_\mathrm{f}\sin\theta_\mathrm{f} & C_\mathrm{f}\cos\theta_\mathrm{f} & -2C_\mathrm{f}\sin 2\theta_\mathrm{f} \end{bmatrix}$$

The last term $\mathbf{C}$ refers to the remaining terms of the series and takes the form

$$\mathbf{C} = \begin{Bmatrix} b_2 \sin 2\theta_0 + \sum_{n=3}^{N}[a_n\cos(n\theta_0) + b_n\sin(n\theta_0)] \\ b_2 \sin 2\theta_\mathrm{f} + \sum_{n=3}^{N}[a_n\cos(n\theta_\mathrm{f}) + b_n\sin(n\theta_\mathrm{f})] \\ 2C_0 b_2\cos 2\theta_0 - C_0\sum_{n=3}^{N} n[a_n\sin(n\theta_0) - b_n\cos(n\theta_0)] \\ 2C_\mathrm{f} b_2\cos 2\theta_\mathrm{f} - C_\mathrm{f}\sum_{n=3}^{N} n[a_n\sin(n\theta_\mathrm{f}) - b_n\cos(n\theta_\mathrm{f})] \end{Bmatrix}$$

In this case the determinant of $\mathbf{M}$ is

$$\Delta = -\frac{C_0 C_\mathrm{f}}{2}[\sin(3\theta_0 - \theta_\mathrm{f}) + 6\sin(\theta_0 + \theta_\mathrm{f}) - \sin(\theta_0 - 3\theta_\mathrm{f}) - 4\sin(2\theta_\mathrm{f}) - 4\sin(2\theta_0)]$$

meaning that the matrix is regular for $C_0 \neq 0$ and $C_\mathrm{f} \neq 0$.

INTERPLANETARY TRAJECTORY DESIGN

The method is tested by designing a fictitious science mission to Ceres, including a sample return phase. The spacecraft departs from the Earth, performs a flyby about Mars and rendez-vous with Ceres. Then, after 400 days of scientific activities it leaves Ceres and returns to the Earth. Figure 4 shows the non-planar trajectory in the ICRF/J2000 frame referred to the ecliptic plane at the reference epoch. The mission is launched on 06-May-2003 (MJD 52765) with a Δv = 1.5 km/s along the velocity vector of the Earth. After 271 days the spacecraft reaches Mars and benefits from a gravity-assist maneuver with v_∞ = 1.59 km/s. The time of flight to Ceres is 862 days, resulting in a total duration of the transfer of 1133 days. The spacecraft reaches Ceres with zero relative velocity (in every direction). Similarly, the CE leg departs and arrives with zero v_∞'s.

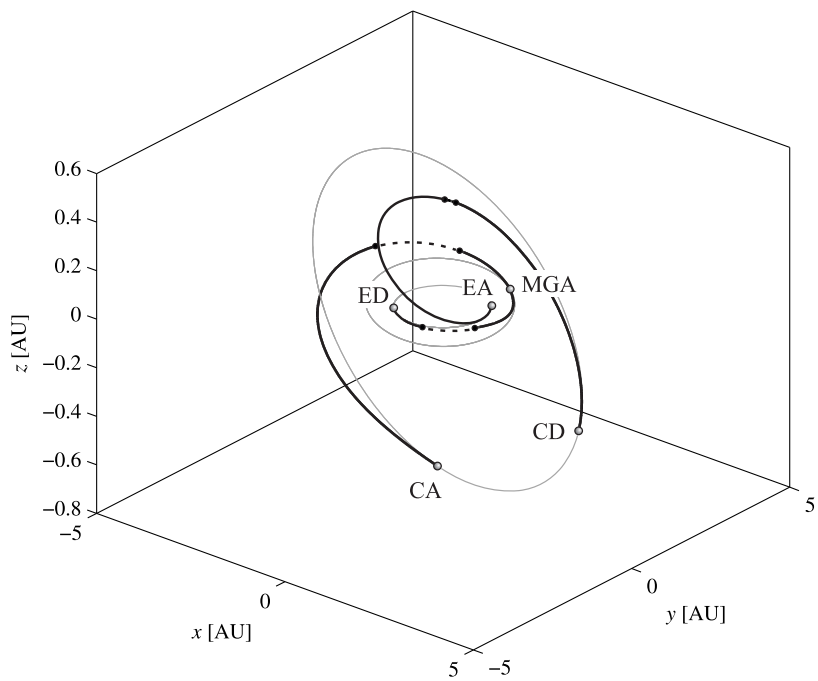

Figure 4: Earth-Mars-Ceres-Earth non-planar transfer. E/M/C refers to Earth, Mars, Ceres, and A/D corresponds to Arrival/Departure. MGA shows the Mars Gravity Assist. Coast arcs are plotted with dashed lines. The out-of-plane component has been exagerated.

Table 1 summarizes the mission, including the times of flight for each leg and the science phase. The total duration of the mission is 2373 days, including the time for operations at Ceres.

Table 1: **Definition of the mission**

Launch v_∞ [km/s]	h_{MGA} [km]	MGA v_∞ [km/s]	t_{EM} [d]	t_{MC} [d]	t_{Science} [d]	t_{CE} [d]
1.50	905.58	1.59	271	862	400	840

The control laws presented in the previous sections provide a flexible method for designing the out-of-plane dynamics. In particular, Fig. 5 displays the transversal component of the acceleration in the EM, MC and CE legs. The trajectories in Fig. 4 have been designed with the polynomial

shaping law, assuming that the first spiral arc and the coast arc are co-planar. This figure also includes the acceleration profile corresponding to the Fourier shaping for the same values of the extra coefficients. The number of coefficients and their values shall be adjusted according to the mission requirements and the geometry of the transfer.

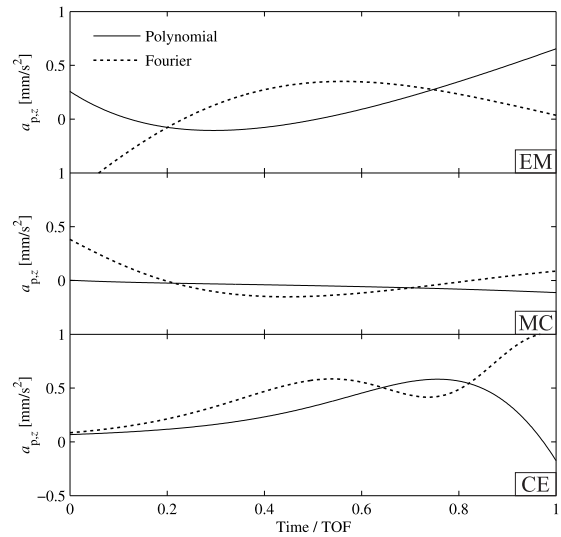

Figure 5: **Out-of-plane acceleration profiles with different steering laws**

CONCLUSIONS

The family of (planar) generalized logarithmic spirals including a control parameter can be extended to account for the out-of-plane motion. By decoupling the in-plane dynamics from the transversal component of the motion the integrals of motion are preserved. Moreover, the equations providing the time of flight are still valid so the dynamics are fully solved in closed-form. This decoupling allows designing different and flexible shaping laws for the out-of-plane dynamics.

The acceleration due to the thrust is solved explicitly and depends on the shaping law. However, the total Δv required for the mission can no longer be integrated in closed-form because of the additional complexity of the equation. The design process decomposes in two phases: first, the planar transfer between the projected orbits is solved; second, the transversal dynamics are solved based on the planar solution.

ACKNOWLEDGEMENT

This work has been carried out at the Jet Propulsion Laboratory within the framework of the JVSRP program. It is part of the research project entitled "Dynamical Analysis, Advanced Orbit Propagation and Simulation of Complex Space Systems" (ESP2013-41634-P) supported by the Spanish Ministry of Economy and Competitiveness. Authors thank the Spanish Government for its support and J. Roa especially thanks "La Caixa" for his doctoral fellowship. They wish to thank J. Senent for his help and advice.

APPENDIX: POLYNOMIAL STEERING LAW

The closed-form solution found for the case of a helix is the simplest that one can obtain. But alternative solutions can be obtained by choosing different steering laws controlling the angle α. Analytic solutions will be obtained as long as Eq. (19) remains integrable in closed-form.

In order to improve the flexibility of the trajectory we introduce the a polynomial approximation

$$\tan\alpha = \sum_{i=0}^{N} c_i\, r^i \tag{26}$$

The coefficients c_i can be chosen at convenience to match certain constraints. Increasing the number of terms N extends the flexibility of the method, at the cost of complicating the form of the analytic

solution. It is barely necessary to mention that $N = 0$ yields the family of helices described in the previous section.

The out-of-plane motion is solved from the integral

$$z(r) = \int \frac{\mathrm{d}z}{\mathrm{d}r}\,\mathrm{d}r = \sum_{i=0}^{N} \left[c_i\, I_i(r) - C_i\right] \tag{27}$$

Here C_i is a constant of integration and $I_i(r)$ denotes the indefinite integral

$$I_i(r) = \int \frac{r^i}{\cos\psi(r)}\,\mathrm{d}r$$

The constant of integration is computed in two different ways, depending on whether the base spiral is $\mathscr{C}$-symmetric or not. Recall that only the elliptic and hyperbolic spirals of Type II are $\mathscr{C}$-symmetric. If the base spiral is $\mathscr{C}$-symmetric then Eq. (27) is replaced by

$$z(r) - z(r_\mathrm{m}) = \sum_{i=0}^{N} c_i\, [I_i(r) - I_i(r_\mathrm{m})] \tag{28}$$

The radius r_m denotes both the radius at apoapsis and periapsis, that share the form $r_\mathrm{m} = [K_2 - 2(1-\xi)]/K_1$. The value of $z(r_\mathrm{m})$ is readily solved by particularizing the previous expression at $t = 0$. For the case of a parabolic or Type I hyperbolic base spiral it is simply

$$z(r) - z(r_0) = \sum_{i=0}^{N} c_i\, [I_i(r) - I_i(r_0)] \tag{29}$$

The integral $I_i(r)$ admits a general closed-form solution for an arbitrary index i, which is

$$I_i(r) = \pm\frac{r^{1+i}}{(1+i)(2+i)\ell}[(1+i)K_1 r F_a + 2(1-\xi)(2+i)F_b]$$

The first sign corresponds to raising regime, and the second to lowering regime. The solution is written in terms of the coefficients F_a and F_b, which are defined in terms of the Appell hypergeometric function* $\mathrm{F}_1(\alpha,\beta_1,\beta_2,\gamma;x,y)$ by

$$F_a = \mathrm{F}_1\left(2+i, \frac{1}{2}, \frac{1}{2}, 3+i, \frac{kK_1 r}{2(1-\xi) - kK_2}, \frac{kK_1 r}{2(1-\xi) + kK_2}\right)$$
$$F_b = \mathrm{F}_1\left(1+i, \frac{1}{2}, \frac{1}{2}, 2+i, \frac{kK_1 r}{2(1-\xi) - kK_2}, \frac{kK_1 r}{2(1-\xi) + kK_2}\right)$$

*In 1882, Appell[12] introduced a generalization of the hypergeometric function in terms of

$$\mathrm{F}_1(\alpha,\beta_1,\beta_2,\gamma;x,y) = \sum_{m=0}^{\infty}\sum_{n=0}^{\infty} \frac{(\alpha)_{m+n}(\beta_1)_m(\beta_2)_n}{m!\,n!\,(\gamma)_{m+n}}\, x^m y^n$$

The terms of the form $(a)_n$ are the Pochhammer symbols, *i.e.*

$$(a)_n \equiv \frac{\Gamma(a+n)}{\Gamma(a)} = a(a+1)\ldots(a+n-1)$$

The coefficient k takes the values $k = +1$ if the base spiral is elliptic ($K_1 < 0$) and $k = -1$ if it is hyperbolic.

In the limit $K_1 \to 0$ the solution $I_i(r)$ reduces to:

$$\lim_{K_1 \to 0} I_i(r) = \frac{2r^{1+i}}{(1+i)\ell}(1-\xi)$$

We emphasize that no approximations have been considered. The polynomial representation of $\tan\alpha$ in Eq. (26) is not an approximate representation, but the assumed shape of the trajectory. Similarly, the solution in Eq. (27) is the exact solution to the motion.

Given this polynomial law for the evolution of $\tan\alpha$ the out-of-plane component of the velocity is simply

$$\frac{\mathrm{d}z}{\mathrm{d}t} = v_{\parallel}\tan\alpha = \sqrt{K_1 + \frac{2(1-\xi)}{r}}\left(\sum_{i=0}^{N} c_i\, r^i\right)$$

This function is differentiated easily to provide the acceleration

$$\frac{\mathrm{d}^2 z}{\mathrm{d}t^2} = \cos\psi \sum_{i=0}^{N} c_i\, r^{i-2}[irv_{\parallel}^2 - (1-\xi)]$$

The transversal component of the thrust acceleration becomes

$$a_{\mathrm{p},z}(r) = \frac{z}{R^3} + \sum_{i=0}^{N} c_i\, r^{i-2}[irv_{\parallel}^2 - (1-\xi)]\cos\psi$$

Note that the expressions for the in-plane components of the motion remain unchanged.

REFERENCES

[1] M. A. Minovitch, "A method for determining interplanetary free-fall reconnaissance trajectories," *JPL Tec. Memo*, Vol. 312, 1961, p. 130.

[2] G. Flandro, "Fast Reconnaissance Missions to the Outer Solar System Utilizing Energy Derived from the Gravitational Field of Jupiter1," *Earth*, Vol. 108, 1966, pp. 6–1.

[3] A. E. Petropoulos and J. A. Sims, "A review of some exact solutions to the planar equations of motion of a thrusting spacecraft," *2nd International Symposium Low Thrust Trajectories, Toulouse, France*, 2002.

[4] R. H. Bacon, "Logarithmic Spiral: An Ideal Trajectory for the Interplanetary Vehicle with Engines of Low Sustained Thrust," *Am J Phys*, Vol. 27, No. 3, 1959, pp. 164–165, 10.1119/1.1934788.

[5] T. Tsu, "Interplanetary travel by solar sail," *ARSJ*, Vol. 29, No. 6, 1959, pp. 422–427, 10.2514/8.4791.

[6] A. E. Petropoulos and J. M. Longuski, "Shape-based algorithm for the automated design of low-thrust, gravity assist trajectories," *J Spacecraft Rockets*, Vol. 41, No. 5, 2004, pp. 787–796, 10.2514/1.13095.

[7] J. Roa, J. Peláez, and J. Senent, "Generalized logarithmic spirals for low-thrust trajectory design," *J Guid Control Dynam*, 2015.

[8] J. Roa and J. Peláez, "Generalized logarithmic spirals for low-thrust trajectory design," *AAS/AIAA Astrodynamics Specialist Conference*, No. 15-729, 2015.

[9] J. Roa and J. Peláez, "Introducing a degree of freedom in the family of generalized logarithmic spirals," *26th Spaceflight Mechanics Meeting*, No. 16-317, 2016.

[10] J. Roa and J. Peláez, "Spiral Lambert's problem with generalized logarithmic spirals," *26th Spaceflight Mechanics Meeting*, No. 16-316, 2016.

[11] M. Barros, "General helices and a theorem of Lancret," *Proceedings of the American Mathematical Society*, Vol. 125, No. 5, 1997, pp. 1503–1509.

[12] P. Appell, "Sur les fonctions hypergéométriques de deux variables," *J Math Pure Appl*, Vol. 8, 1882, pp. 173–216.